

Rapid hydration and weakening of anhydrite under stress: Implications for natural hydration in the Earth's crust and mantle

Johanna Heeb^{1,2}, David Healy¹, Nicholas E. Timms², Enrique Gomez-Rivas³

5 Supplement S

Alternative sample names:

Ò1	Ò2	Ò3	Ò4	Ò5	Ò6	Ò7	Ò8	V
BA-3	BA-4	AA-5	BA-1	BA-2	BA-5	AA-2	AA-3	V3-5

Figures

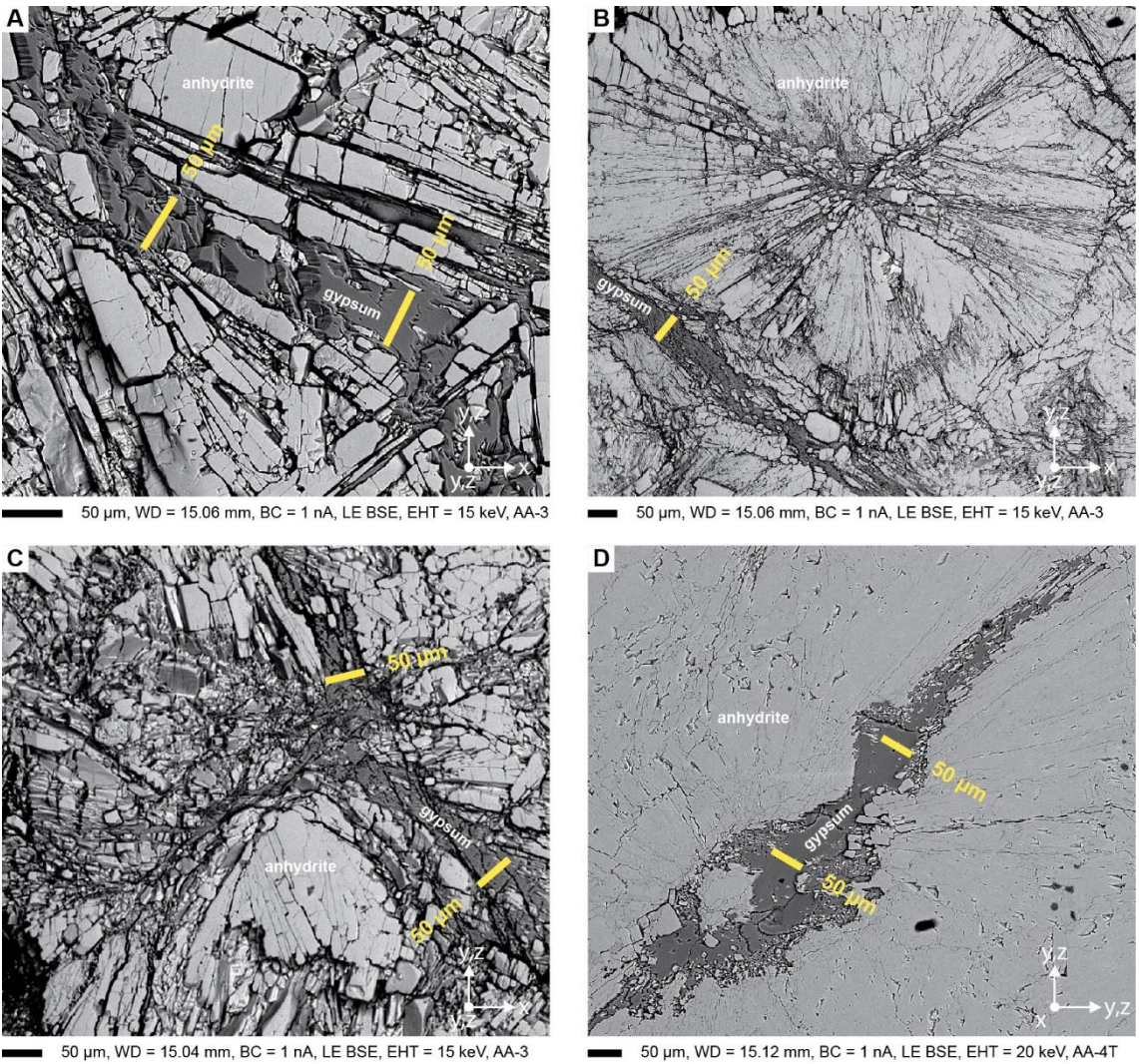
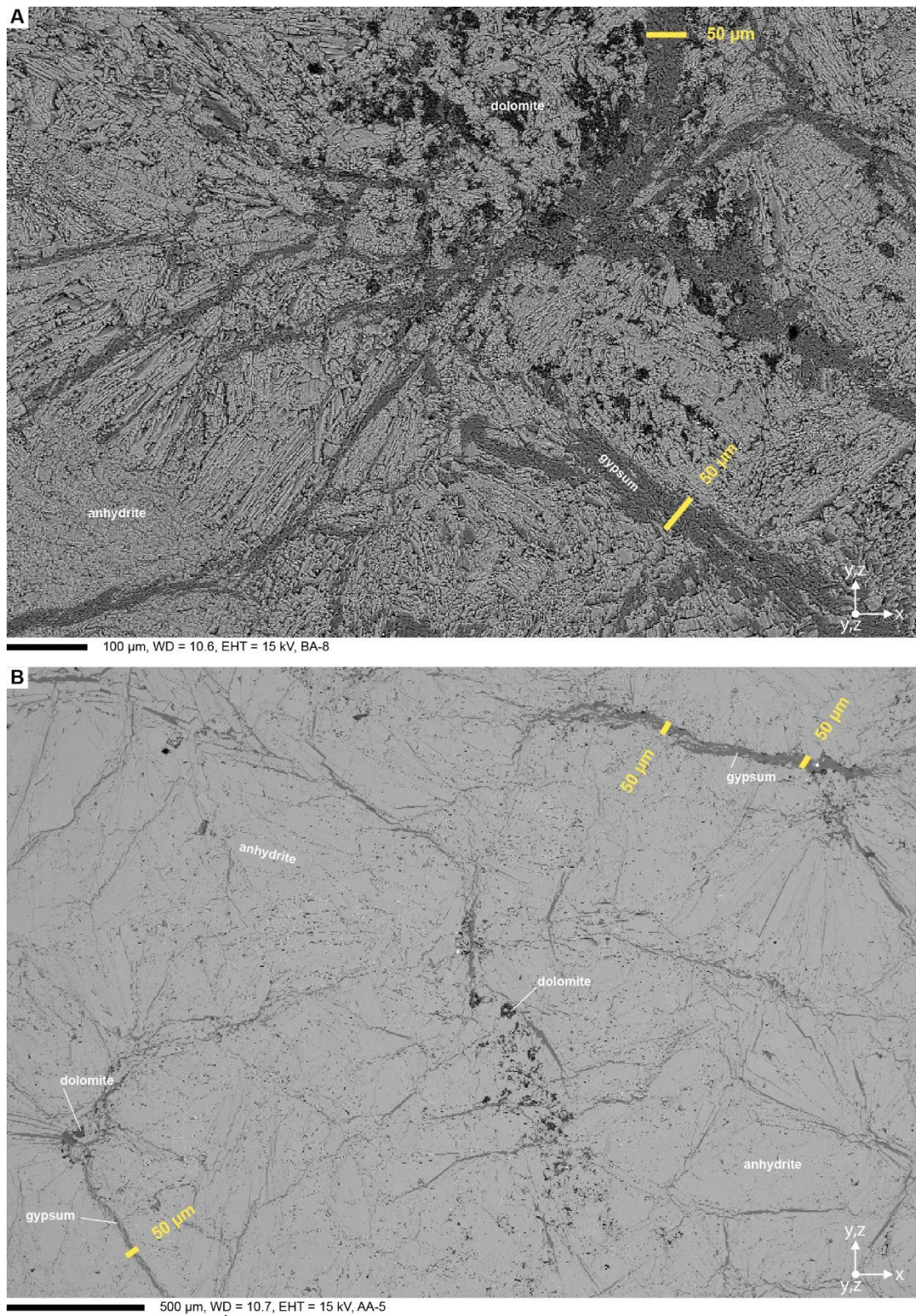


Fig. S1: Electron backscatter images of Òdena anhydrite. A: gypsum vein in anhydrite, sample Ò8. B: Gypsum vein next to a spherulite with gypsum in the centre and between grains, sample Ò8. C: Gypsum vein in anhydrite, sample Ò8. D: Gypsum vein cutting through spherulites, sample not used for experiments.



15 Fig. S2: Electron backscatter maps of Odena anhydrite. A: Gypsum vein systems, sample not used for experiments. B: Map of sample 03.

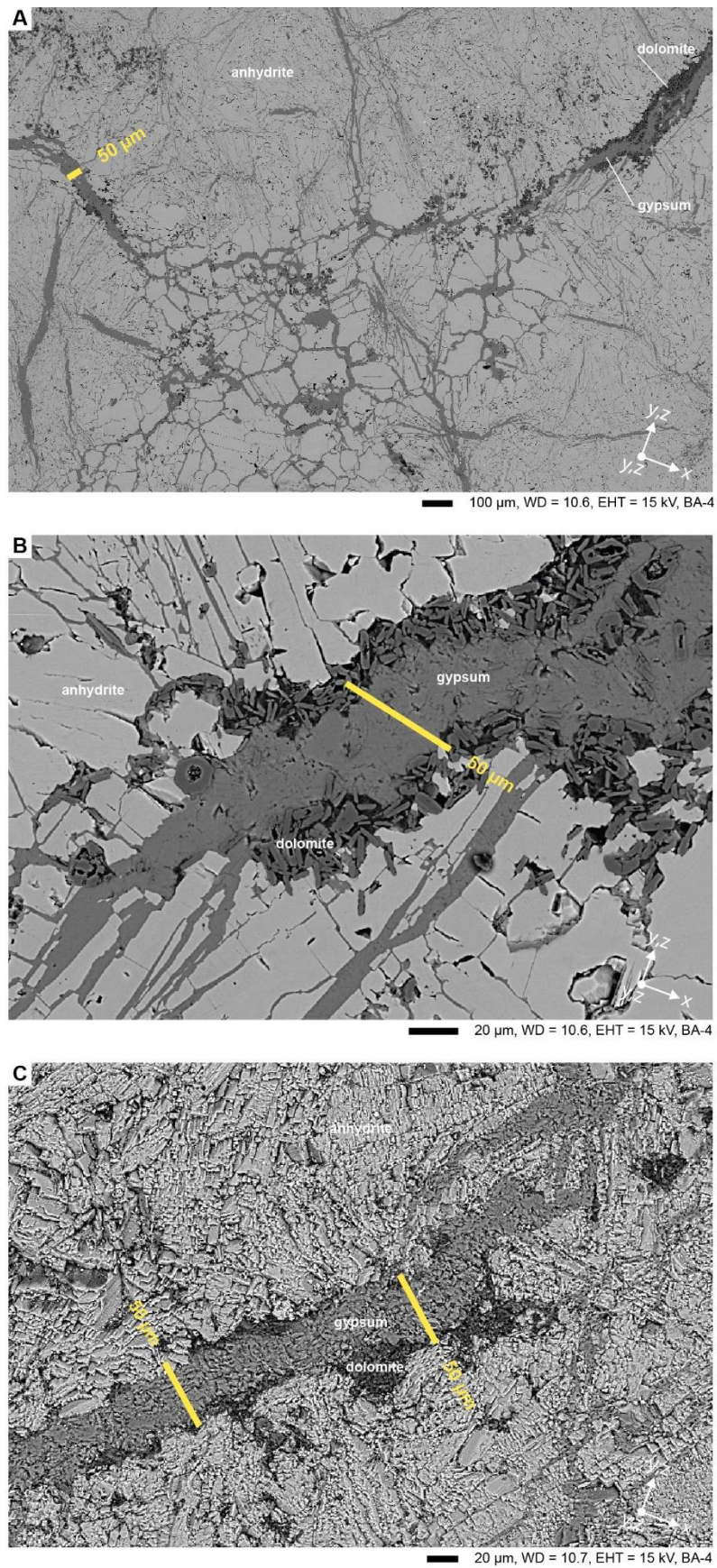


Fig. S3: Electron backscatter images of Òdena anhydrite sample 02.

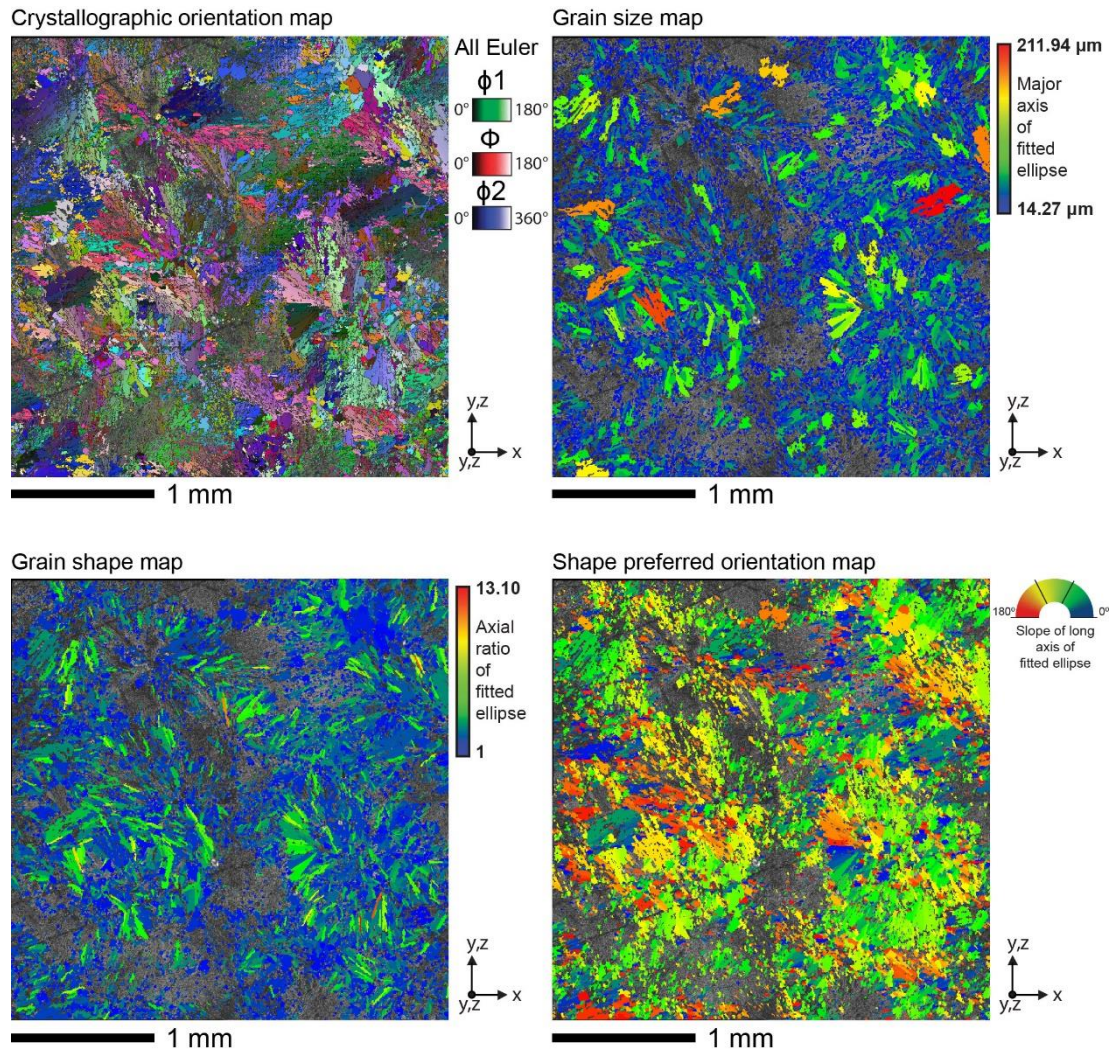


Fig. S4: Electron backscatter diffraction analysis of initial Òdena anhydrite sample material. See Fig. 2c) and d) for IPF_x EBSD map and equal area, lower hemisphere pole figures of anhydrite. Step size was 4 μm .

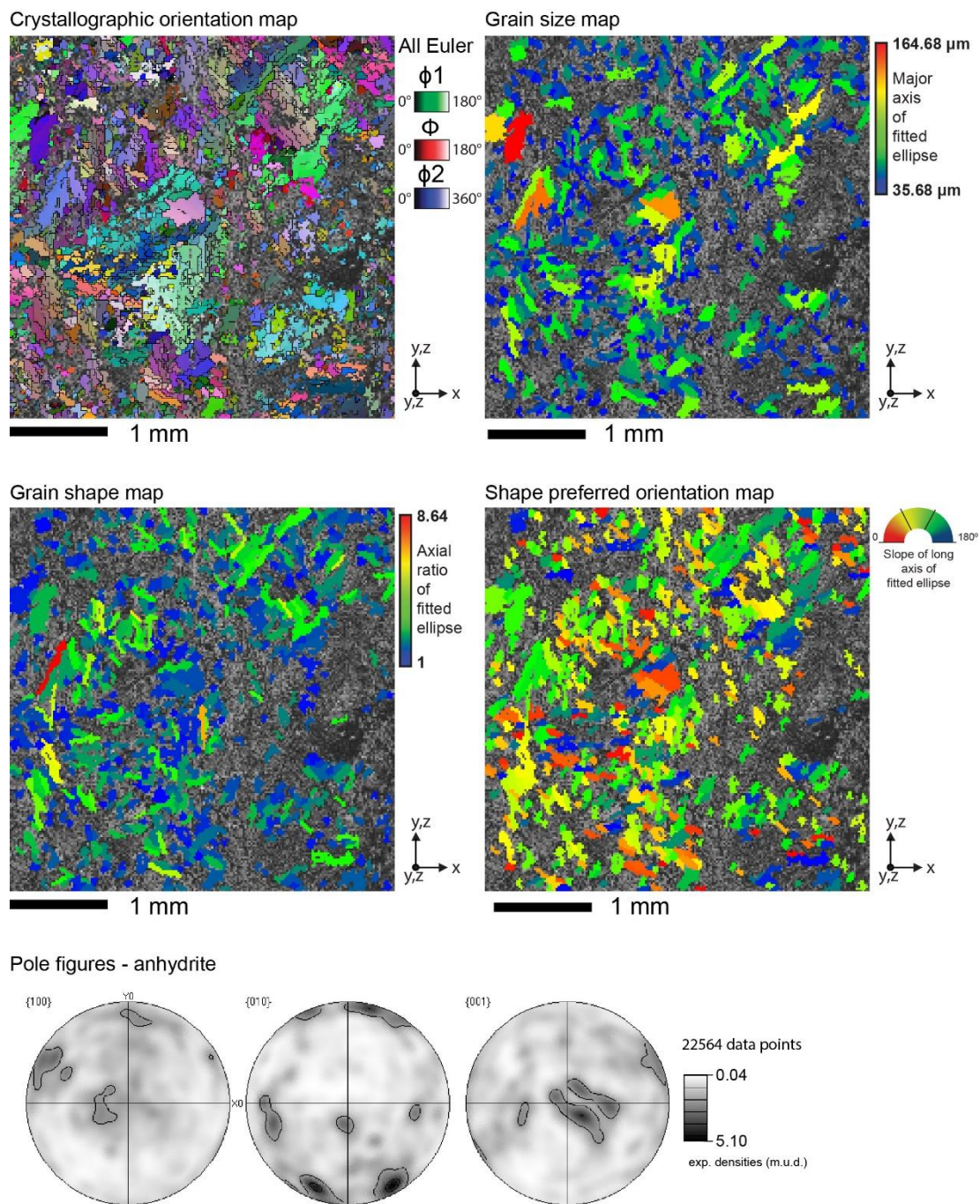


Fig. S5: Electron backscatter diffraction analysis of initial Ödena anhydrite sample material, including equal area, lower hemisphere pole figures of anhydrite. Step size was 10 μm .

30

35

40 Ò1 (BA-3, ssdc)



Ò3 (AA-5, 'wet')



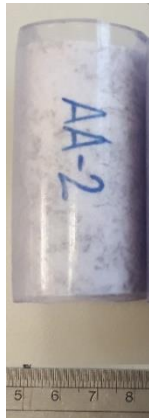
Ò4 (BA-1, 'wet')



Ò5 (BA-2, 'wet')



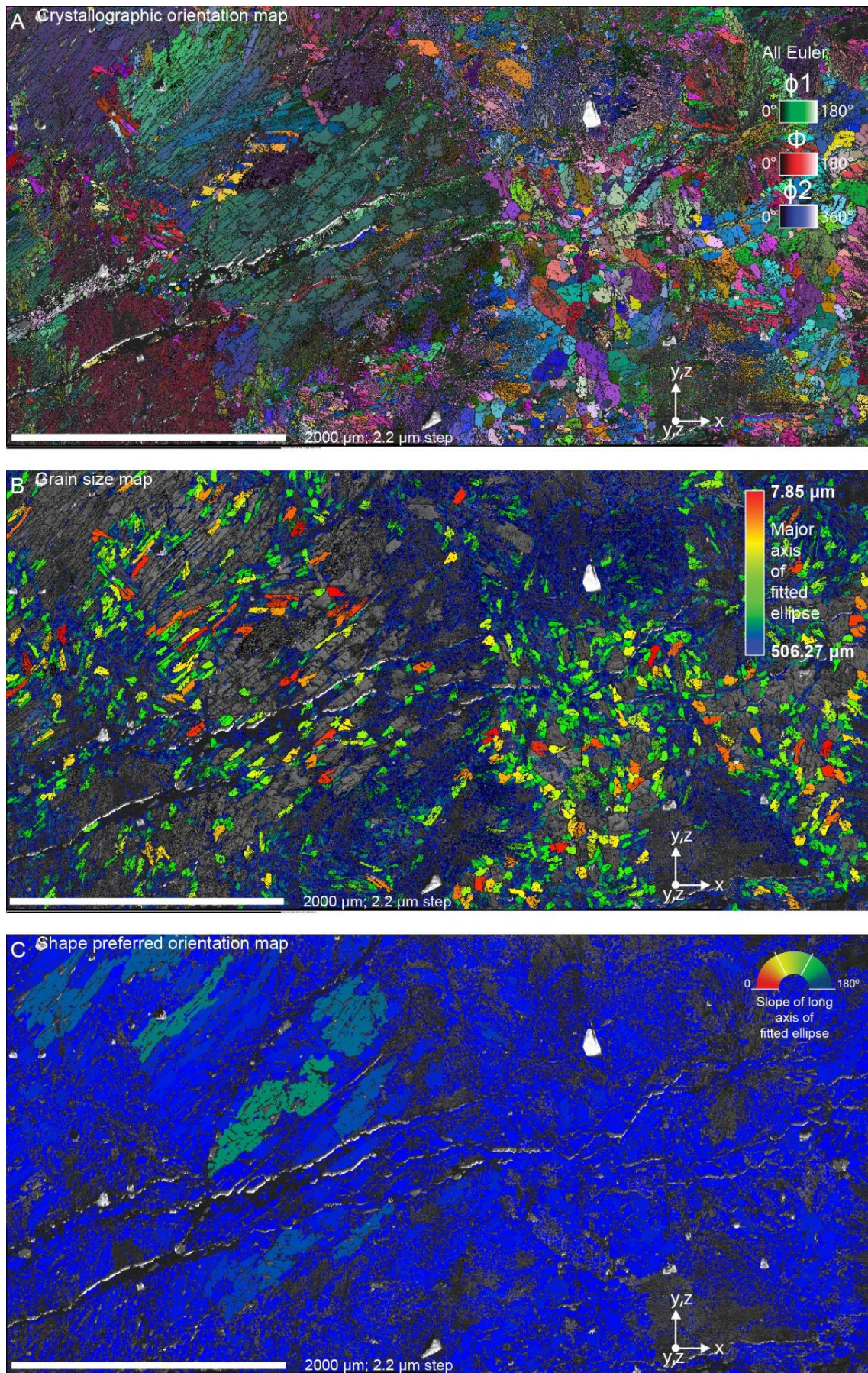
Ò7 (AA-2, dry)



V (V3-5, dry)

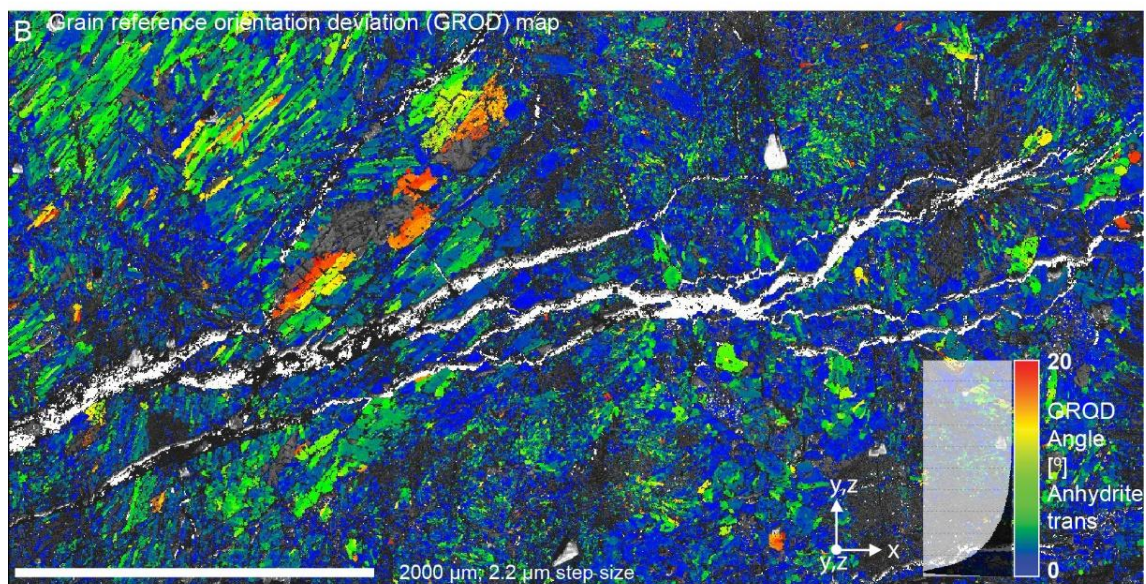
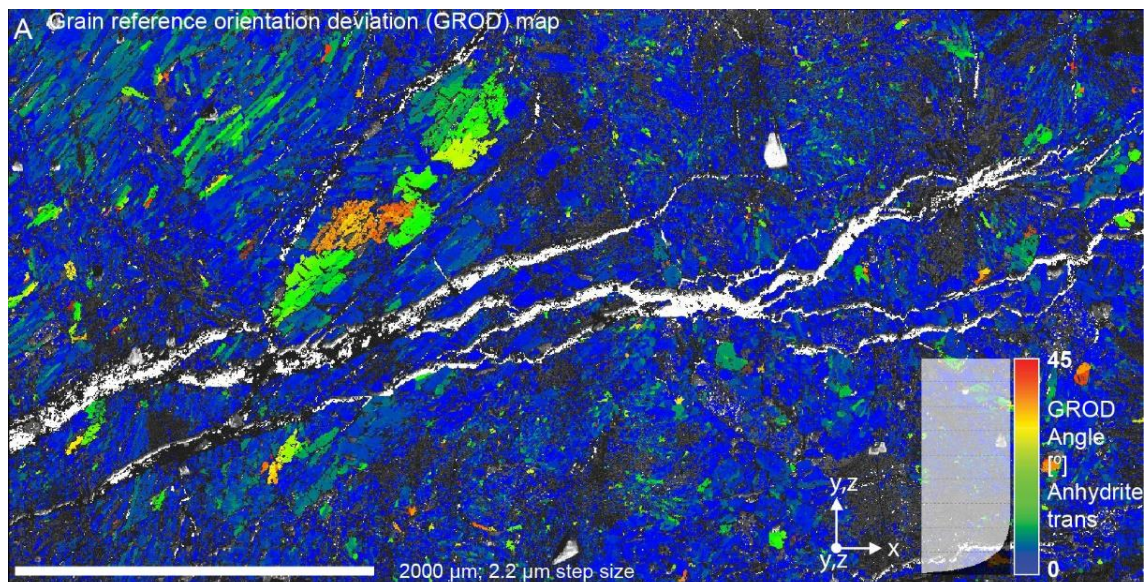


Fig. S6: Photographs of post-experiment cores after undergoing all three test modes.



$$\sigma_1 \rightarrow \leftarrow \sigma_1$$

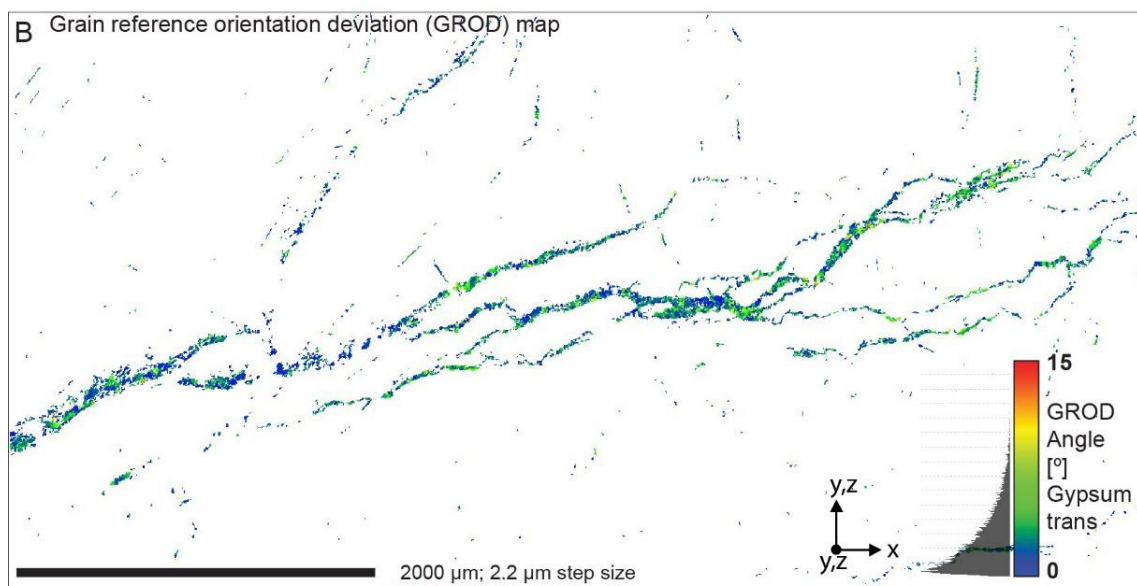
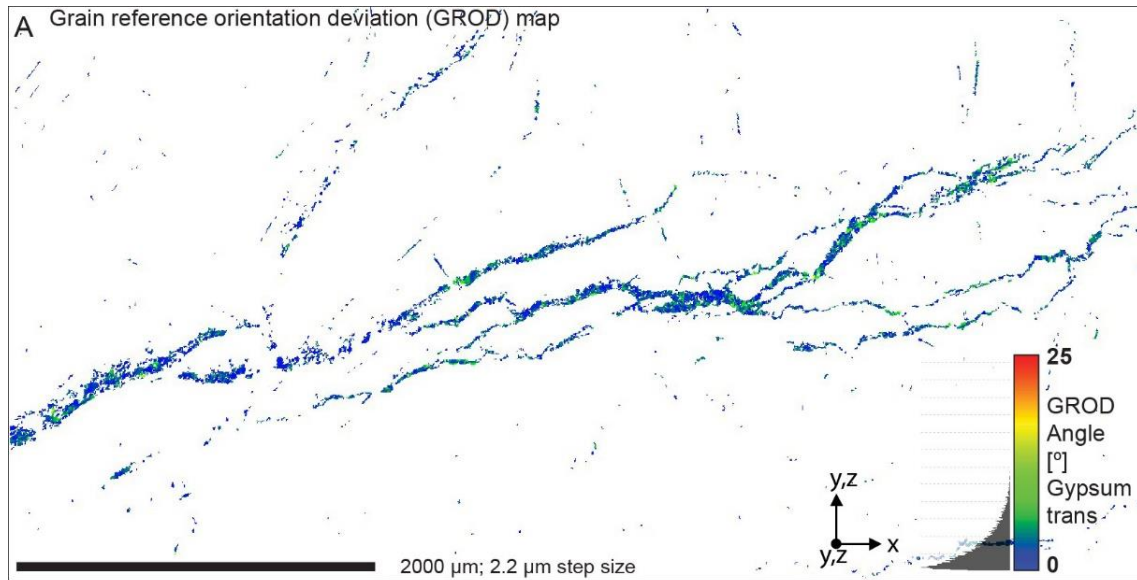
Fig. S7: Additional electron backscatter diffraction analysis from the area of sample O3 ('wet' mode experiment).



$$\sigma_1 \rightarrow \leftarrow \sigma_1$$

Fig. S8: Grain reference orientation deviation (GROD) maps of anhydrite from the Area 1 electron backscatter diffraction dataset of Ö3 ('wet' mode experiment). GROD analysis shows orientation heterogeneities that form during deformation, and hence displays internal deformation of grains. Each pixel is coloured based on the misorientation of the point relative to a reference orientation for the grain to which the point belongs to. Component limits (GROD angle) were at a range of 0 to 45° for A and to 0 to 20° for B. Exclusion of higher angles results in loss of data and is more sensitive to low angle heterogeneities.

GROD analysis shows that the blocky area has slightly higher internal deformation, with angles ~40° in one large grain and ~20° in surrounding grains. The rest of the anhydrite appears heterogeneous, with GROD angles commonly between 0 and 15°.

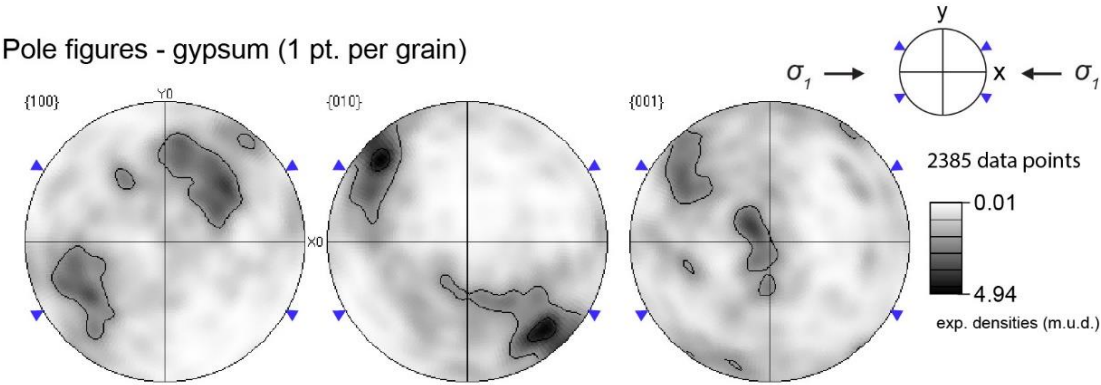


$$\sigma_1 \rightarrow \leftarrow \sigma_1$$

60 **Fig. S9: Grain reference orientation deviation (GROD) maps of vein-hosted gypsum from the Area 1 electron backscatter diffraction dataset of Ò3 (post ‘wet’ mode experiment). Component limits (GROD angle) were at a range of 0 to 25° for A and to 0 to 15° for B. Exclusion of higher angles results in loss of data and is more sensitive to low angle heterogeneities.**

Summary grain statistics

			no grains	Grains%	Area	%	AVG d	STDV d	AVG slope	STDV slop	AVG AR	STDV AR
anh	2	23453	23452	90.76905	1.03E+07	9.508E+01	16.86657	16.54946	84.1283	51.02407	2.082103	0.896492
gyp	23454	25838	2385	9.230948	5.33E+05	4.923E+00	14.70951	8.242795	74.57741	49.84299	2.15751	1.020427
total			25837		1.08E+07							
EX	16.62	Average, expectation										
D²X	249.65	Variance, dispersion										
s	15.8	Standard deviation										
s/EX	0.95066	Coefficient of variation										
Xmin	7.8501	Minimum value										
Xmax	506.27	Maximum value										
N	25760	Size of the data set										



65

Fig. S10: Grain statistical data and one point per grain, equal area, lower hemisphere pole figures of gypsum from analysis of the electron backscatter diffraction data set of Area 1 in sample Ò3 (post ‘wet’ mode experiment).

70

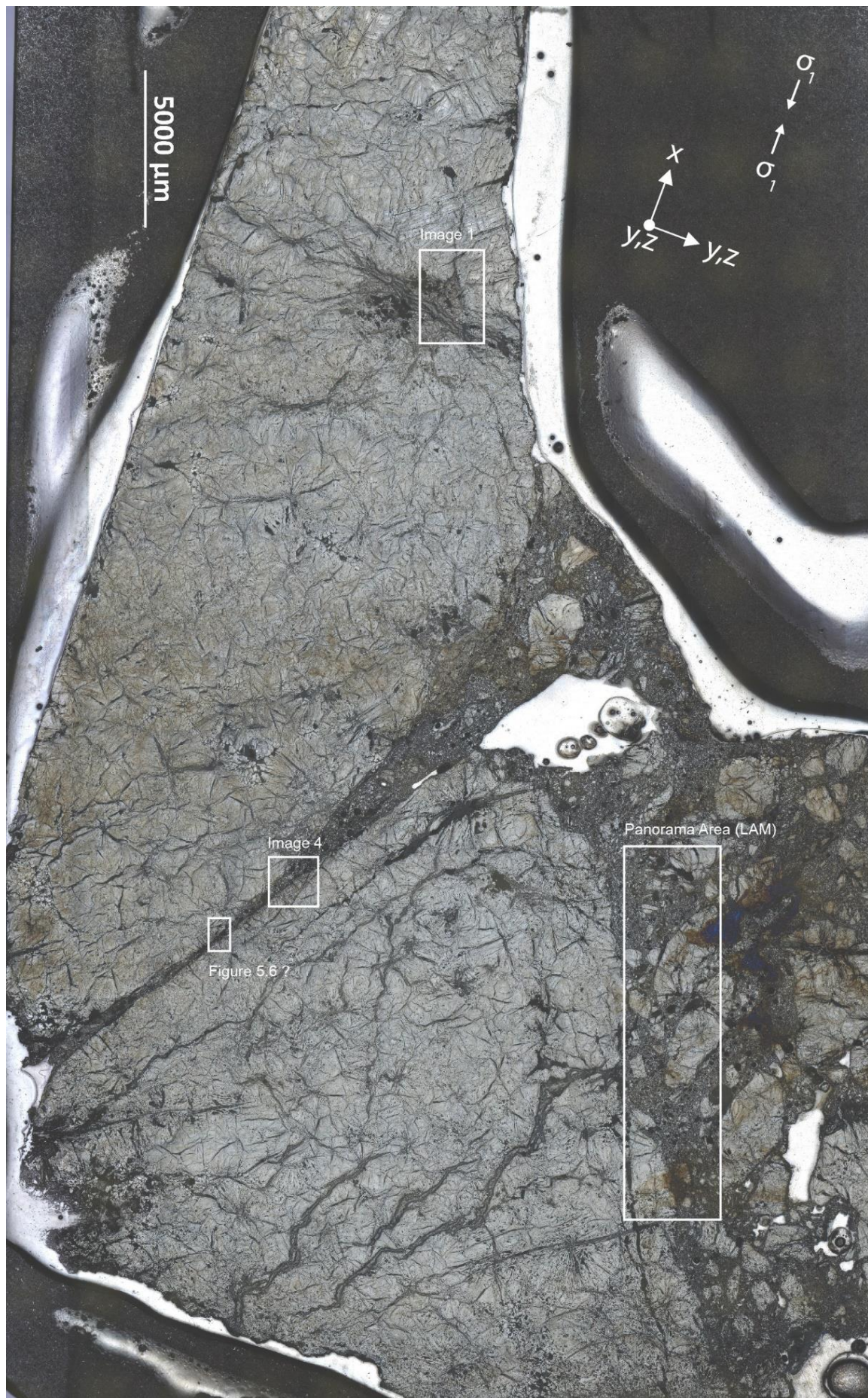


Fig. S11: Reflected light microscopy images of a thin section of sample 02 (post ssdc mode experiment) with areas marked where further analysis was done. The area marked as Figure 5.6? is an estimate, as the thin section was polished for EBSD between imaging.

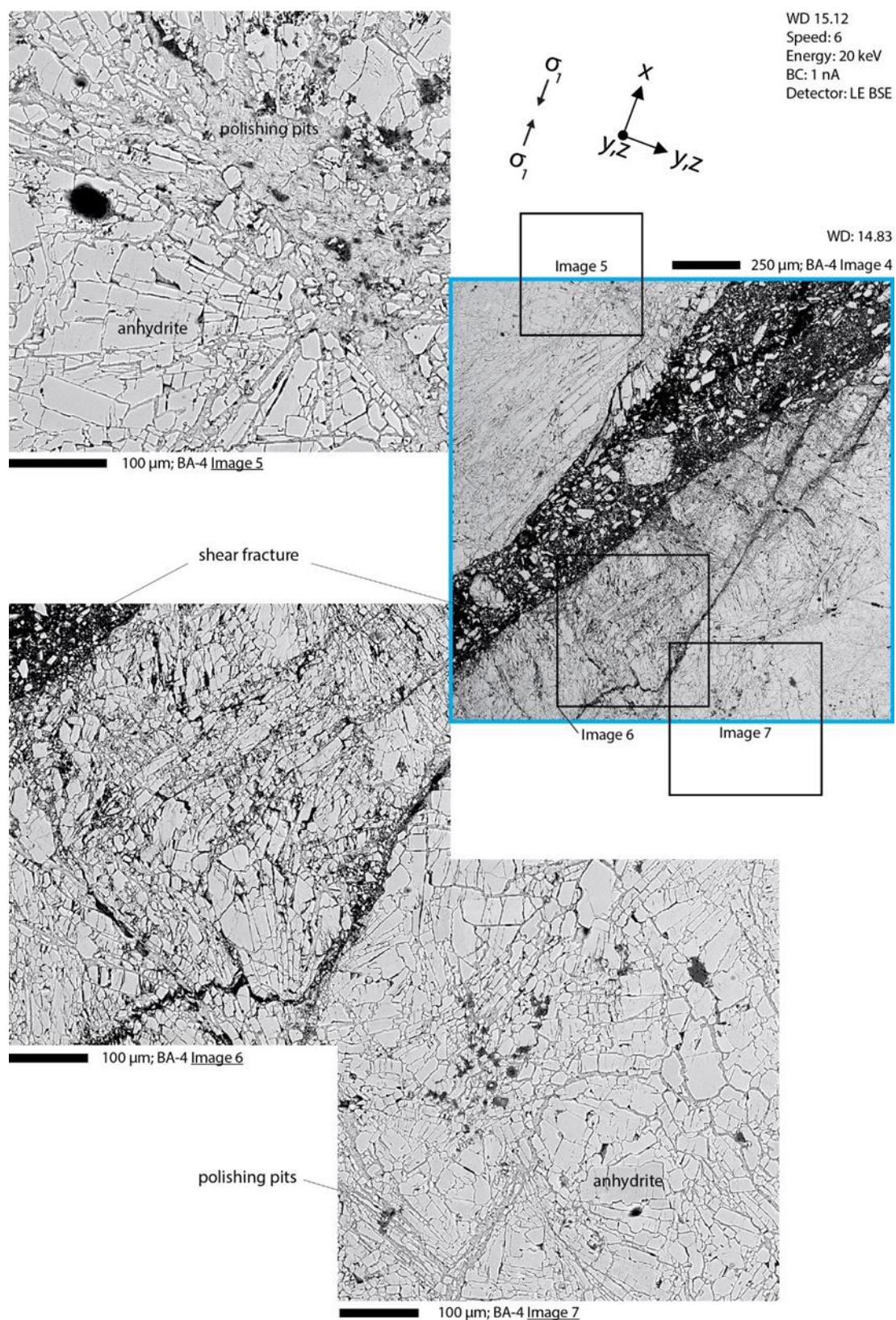
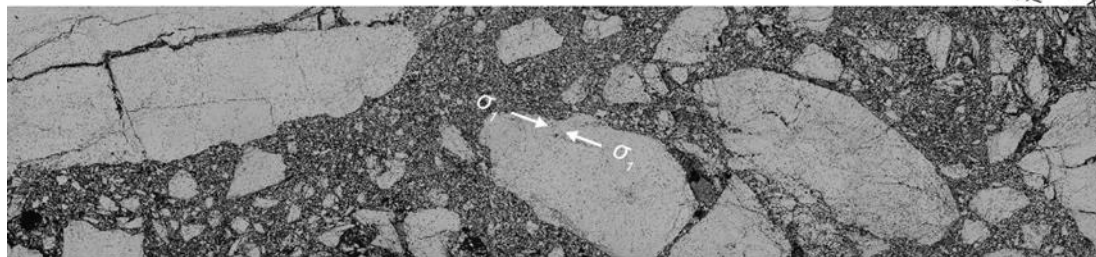


Fig. S12: Backscatter electron images of O₂ after ssdc. Image 4: shear fracture map, location marked in Figure S11. Image 5: ~ 100 μm wide polishing pit (gypsum vein that lost gypsum due to polishing), and spherulitic radial anhydrite laths. Image 6: cataclastic zone with shear bands between the open shear fracture (no matrix, filled with clasts). A long fracture divides the cataclastic zone (Image 6) from the intact fabric of Image 7.

A

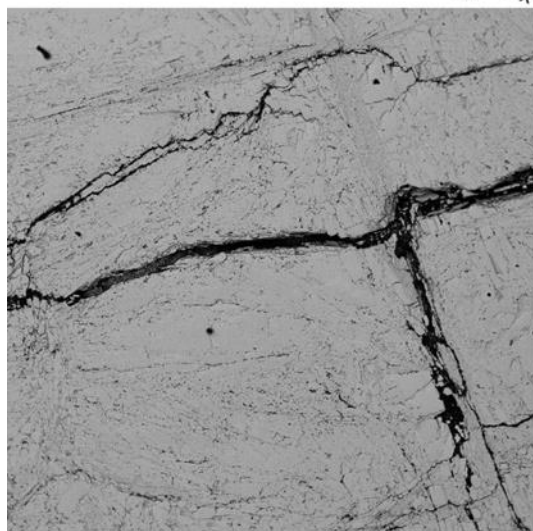
Panorama Area



1 mm; WD 15.35 mm

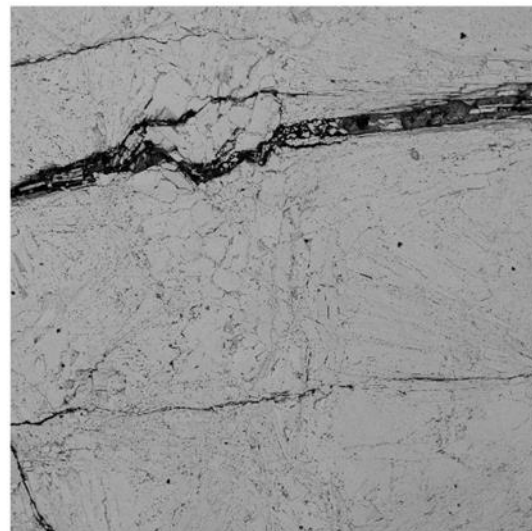
B

LAM Area1_0_0



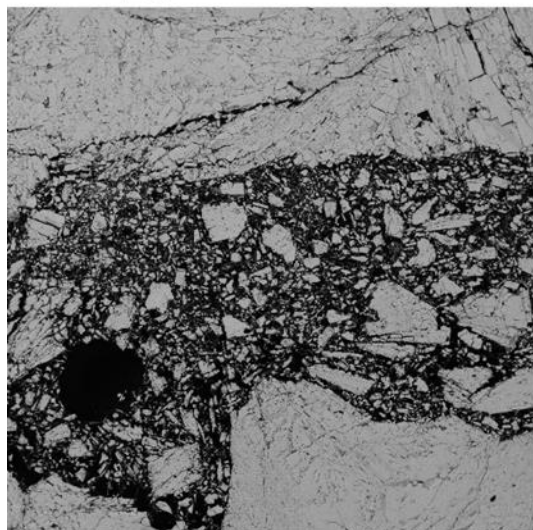
500 μ m; WD 15.35 mm

LAM Area1_1_0



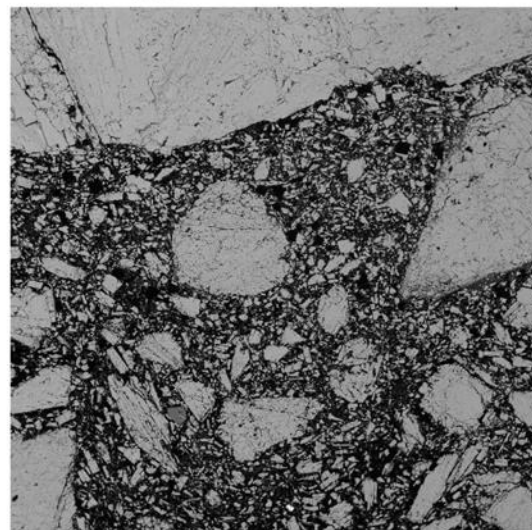
500 μ m; WD 15.35 mm

LAM Area1_0_1



500 μ m; WD 15.35 mm

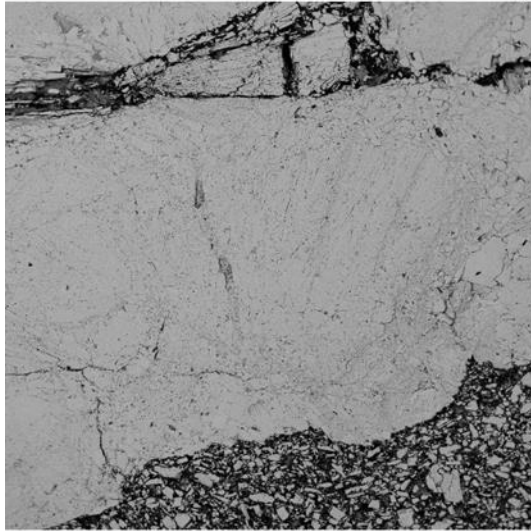
LAM Area1_1_1



500 μ m; WD 15.35 mm

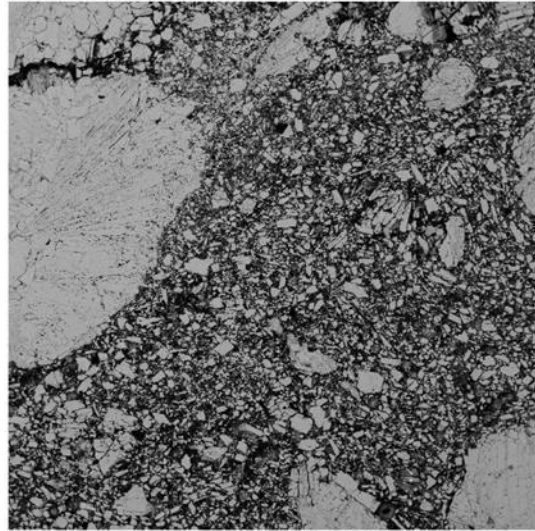
C

LAM Area1_2_0



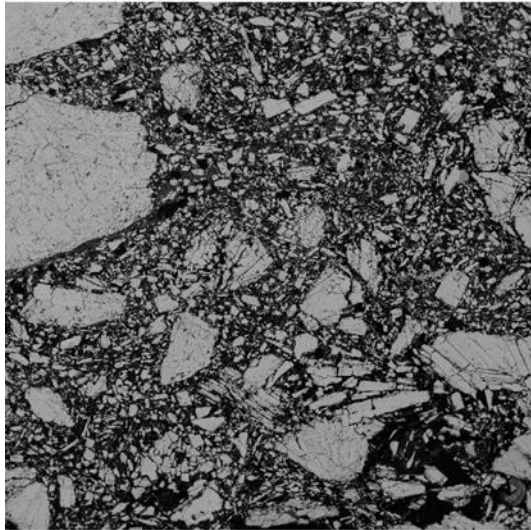
500 μ m; WD 15.35 mm

LAM Area1_3_0



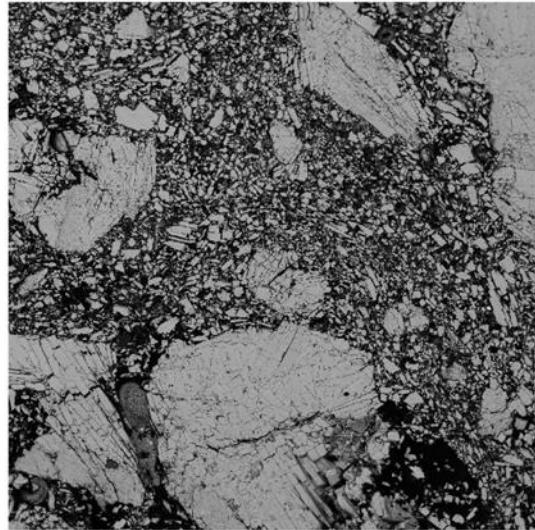
500 μ m; WD 15.35 mm

LAM Area1_2_1



500 μ m; WD 15.35 mm

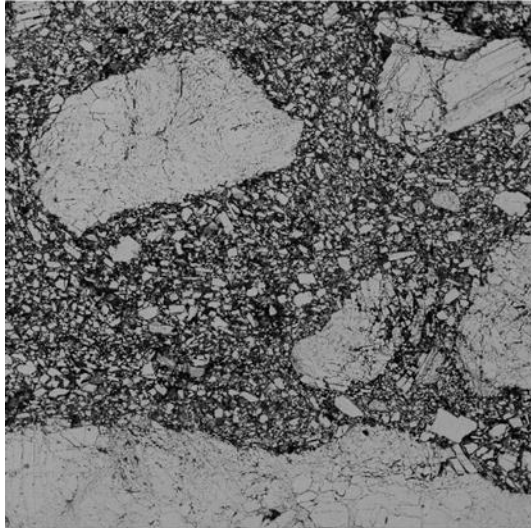
LAM Area1_3_1



500 μ m; WD 15.35 mm

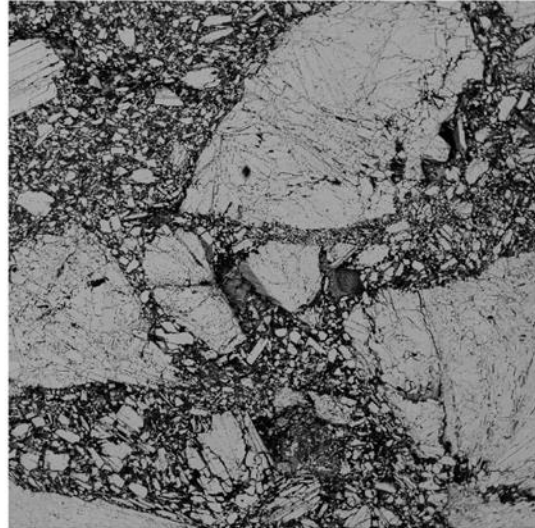
D

LAM Area1_4_0



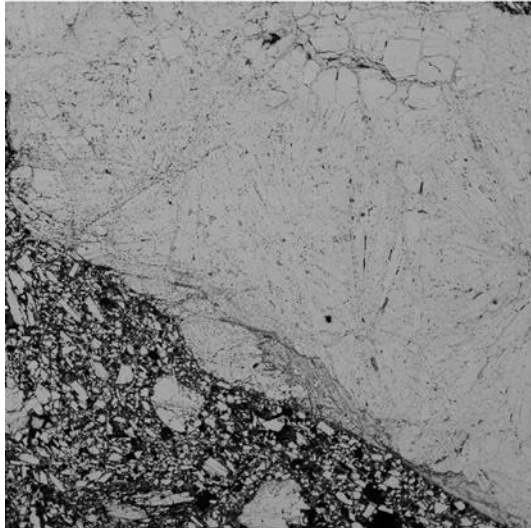
500 μ m; WD 15.35 mm

LAM Area1_5_0



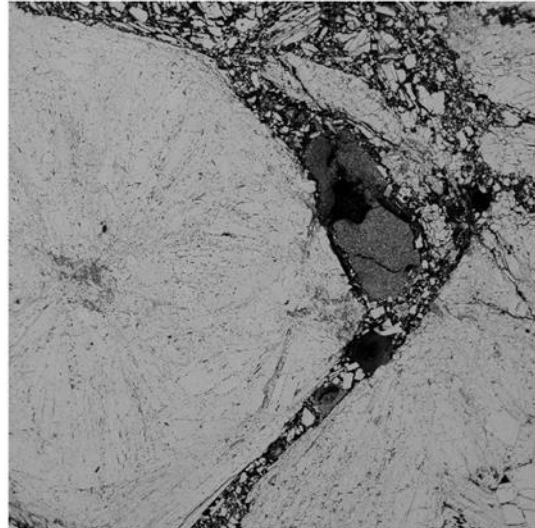
500 μ m; WD 15.35 mm

LAM Area1_4_1



500 μ m; WD 15.35 mm

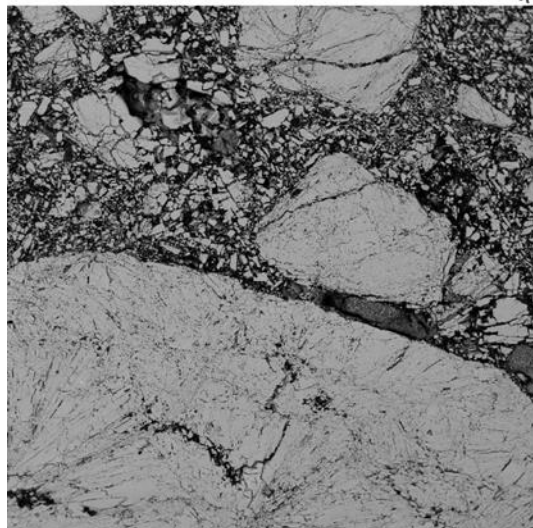
LAM Area1_5_1



500 μ m; WD 15.35 mm

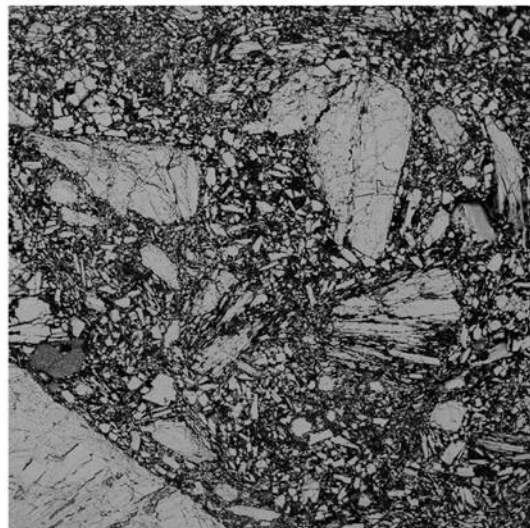
E

LAM Area1_6_0



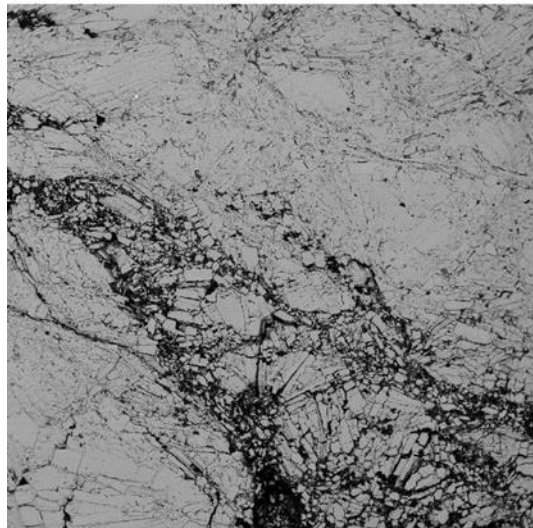
500 μm ; WD 15.35 mm

LAM Area1_7_0



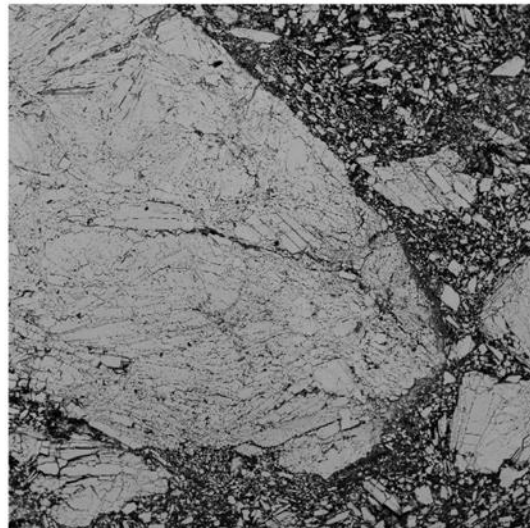
500 μm ; WD 15.35 mm

LAM Area1_6_1



500 μm ; WD 15.35 mm

LAM Area1_7_1



500 μm ; WD 15.35 mm

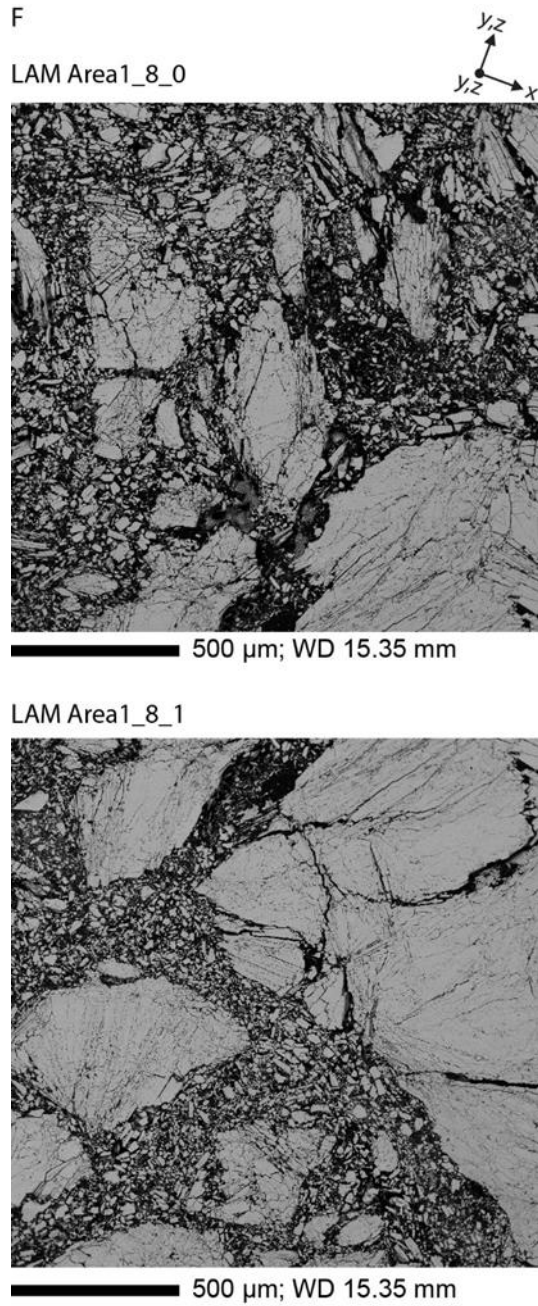
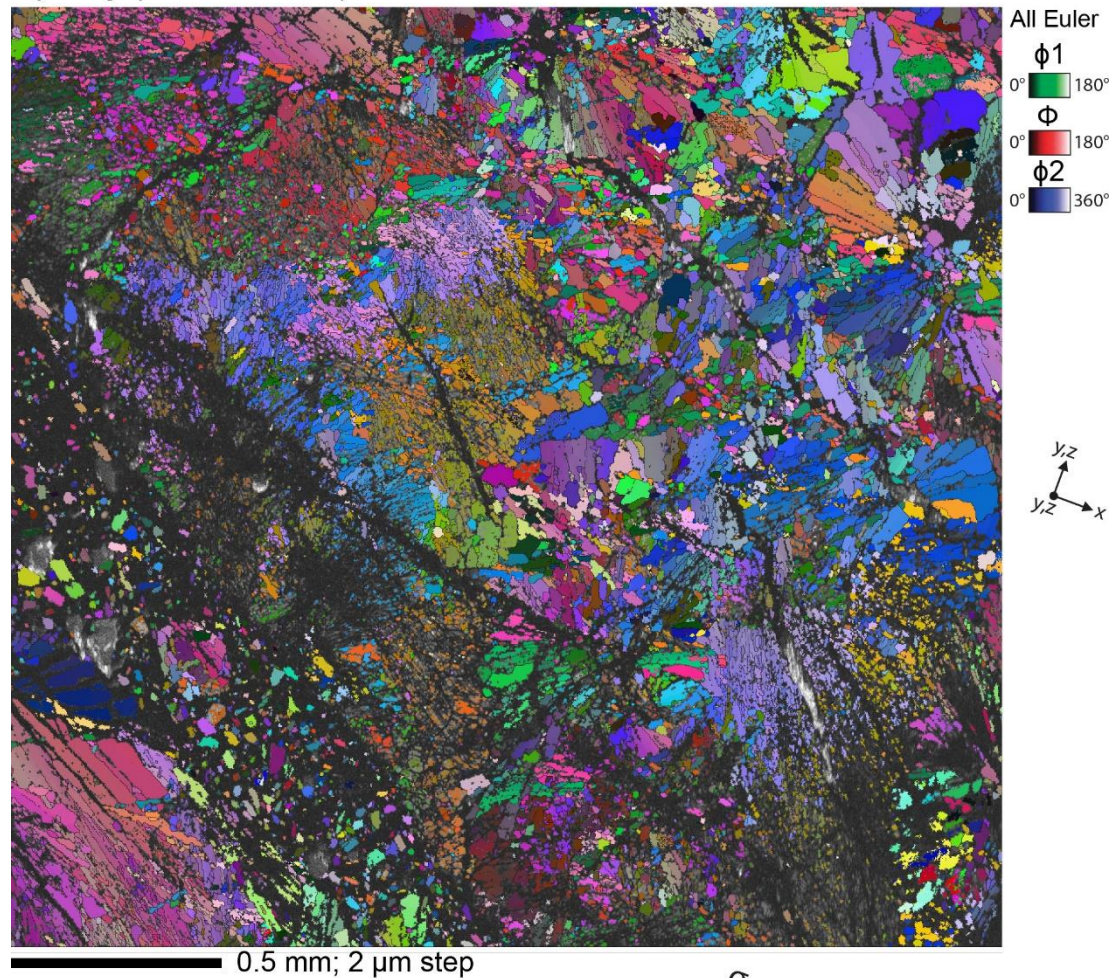


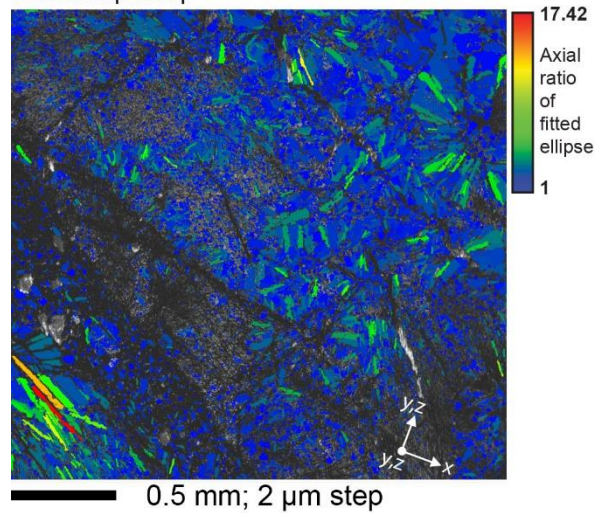
Fig. S13: Backscatter electron panorama of a cataclastic shear zone in Ö2 after steady state differential compaction. A: Panorama, B to F single panorama frames. Light grey: anhydrite, medium grey: gypsum, black: open fractures. A mixed matrix of < 100 µm sized gypsum and anhydrite particles contains up to millimetre-scale anhydrite clasts with intense internal fracturing and low gypsum content. The amount of gypsum is difficult to identify from the images, as the sample lost gypsum due to polishing. The location of the panorama is marked as Panorama Area (LAM) in Figure A11.

95

Crystallographic orientation map



Grain shape map



Shape preferred orientation map

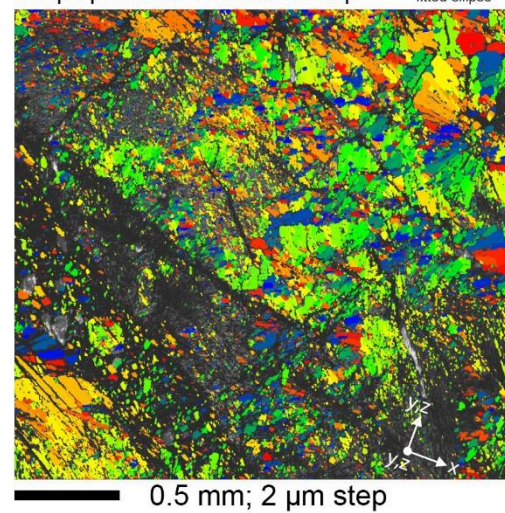


Fig. S14: Electron backscatter diffraction analysis of a cataclastic shear zone and surrounding fabric with spherulites in sample Ö2 after steady state differential compaction. Gypsum was not detected, due to polishing pits.

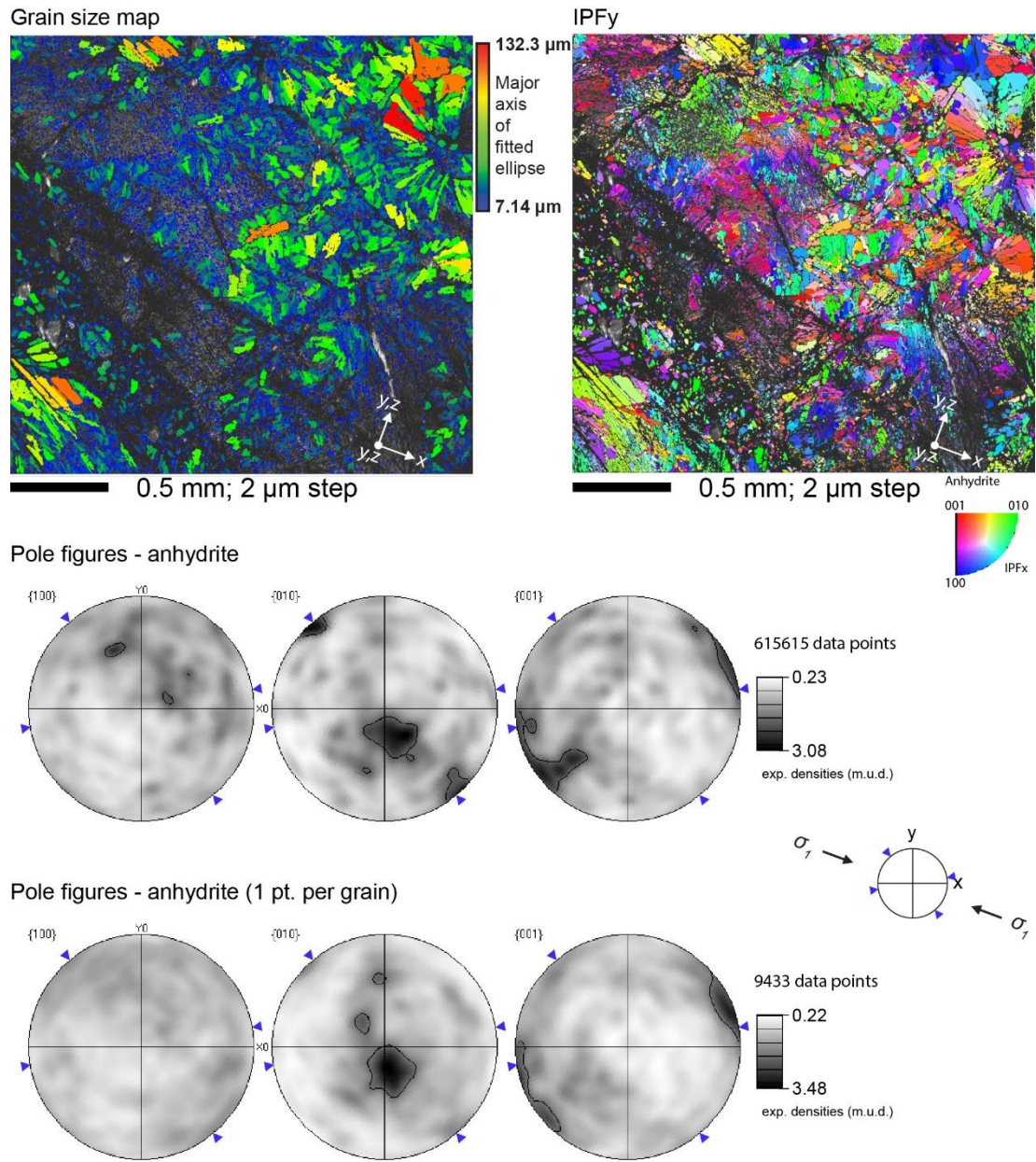
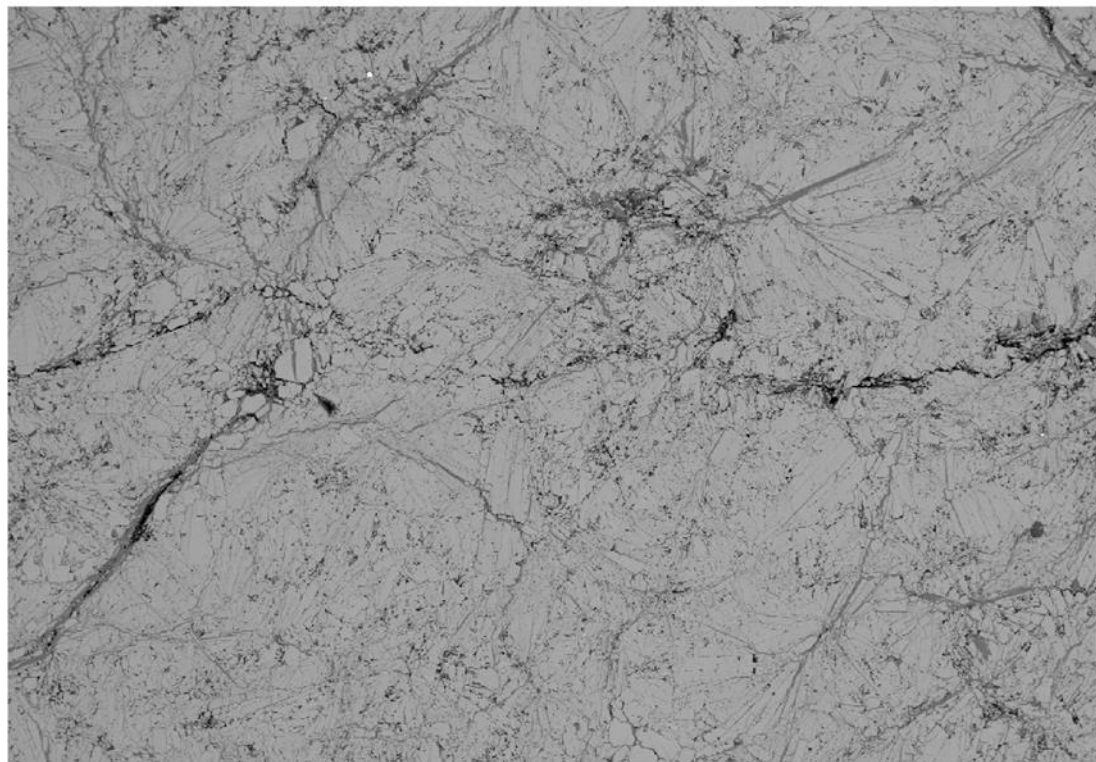


Fig. S15: Second part of backscatter diffraction analysis of a cataclastic shear zone in sample 02. Equal area, lower hemisphere pole figures of anhydrite based on the complete dataset and based on 1 point per grain subset.

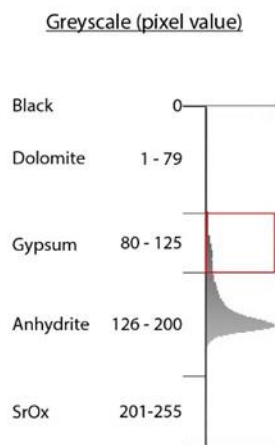
A



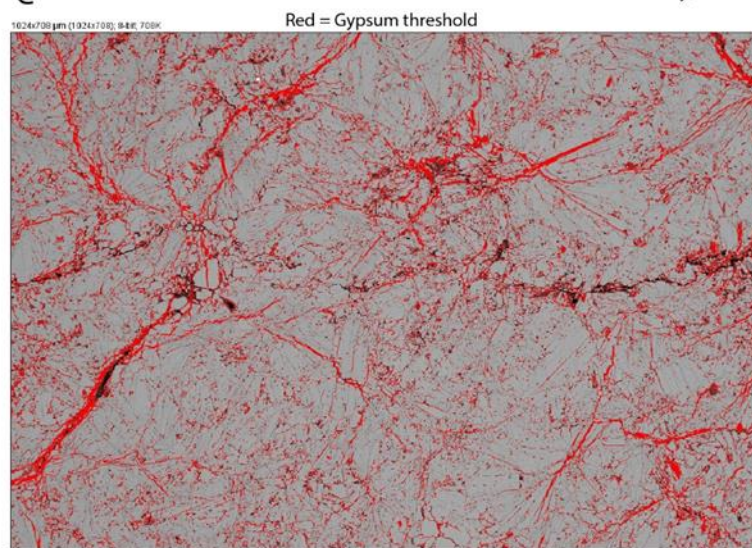
500 µm; WD = 10.7 mm; 15.00 kV; Image 2



B



C



500 µm; WD = 10.7 mm; 15.00 kV; Image 2

Fig. S16: Phase content analysis via greyscale threshold (ImageJ) from A: backscatter electron Image 2 of Òdena quarry sample Ò8 (AA-3). This sample went through a dry mode test and no signs of new formed gypsum was found. B: Greyscale threshold settings defined to quantify %. SrOx = accessory phases. C: Image 2 with all pixels that fall into the gypsum threshold in red. See table A1 for further results.

110

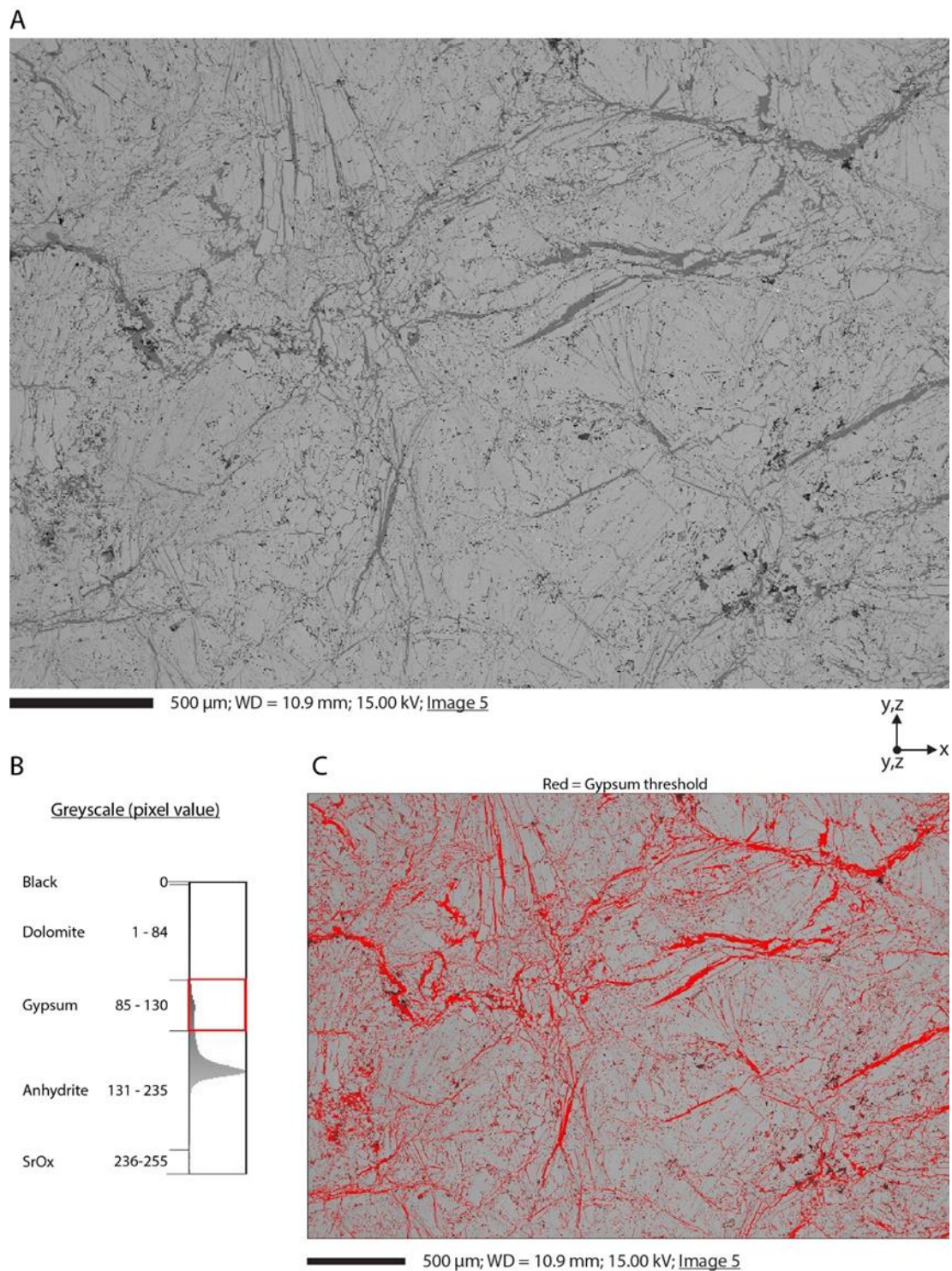
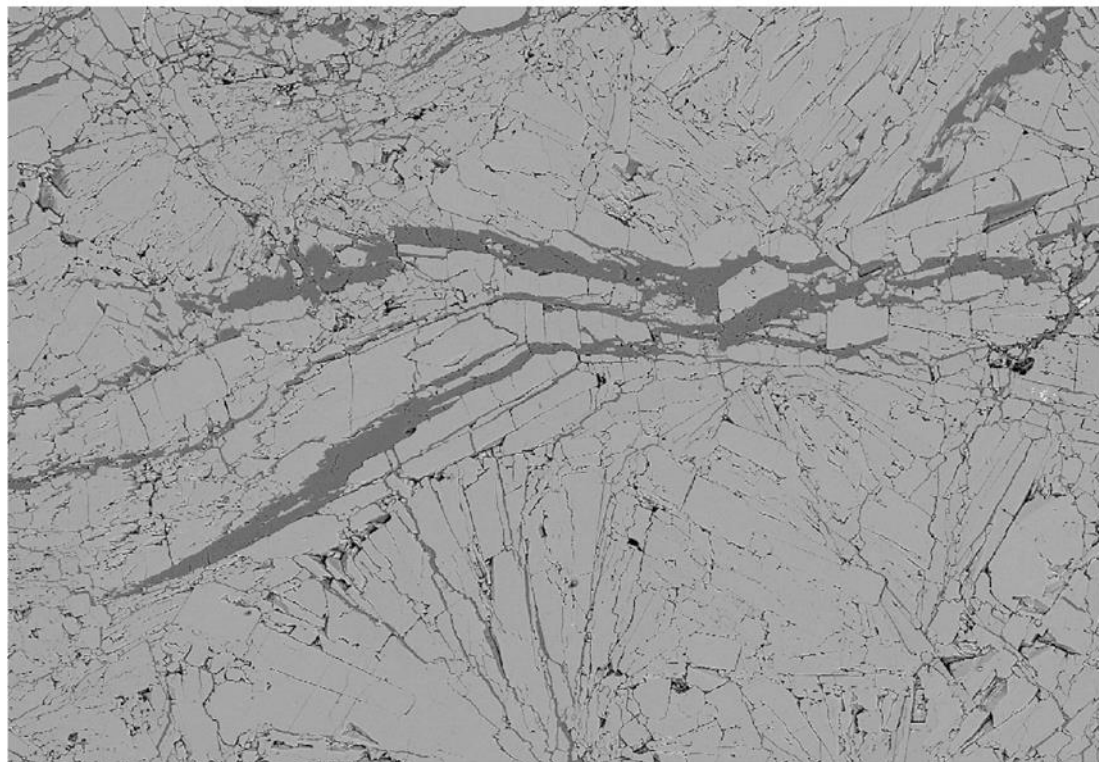
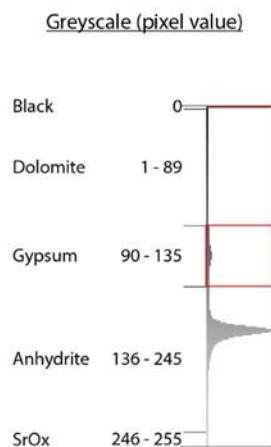


Fig. S17: Phase content analysis via greyscale threshold (ImageJ) from A: backscatter electron Image 5 of Òdena quarry sample Ò8 (AA-3). B: Greyscale threshold settings defined to quantify %. SrOx = accessory phases. C: Image 5 with all pixels that fall into the gypsum threshold in red. See table A1 for further results.

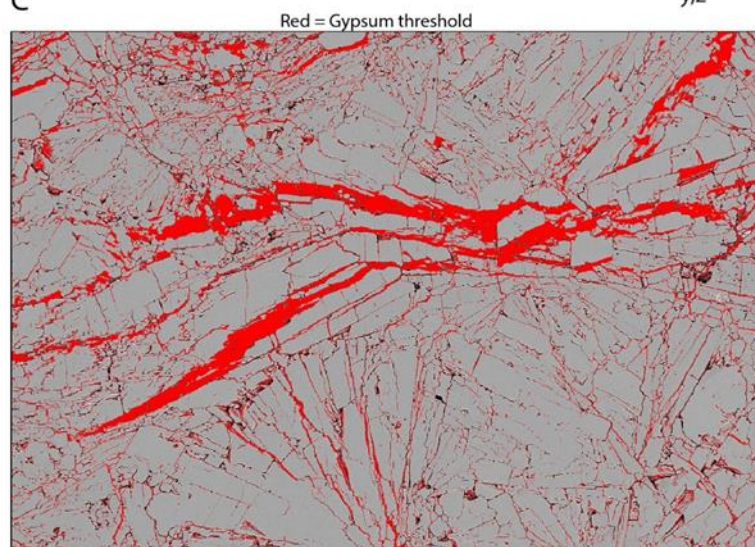
A



B



C



250 µm; WD = 10.9 mm; 15.00 kV; Image 6

Fig. S18: Phase content analysis via greyscale threshold (ImageJ) from A: backscatter electron Image 6 of Òdena quarry sample Ò8 (AA-3). B: Greyscale threshold settings defined to quantify %. SrOx = accessory phases. C: Image 6 with all pixels that fall into the gypsum threshold in red. See table A1 for further results.

120

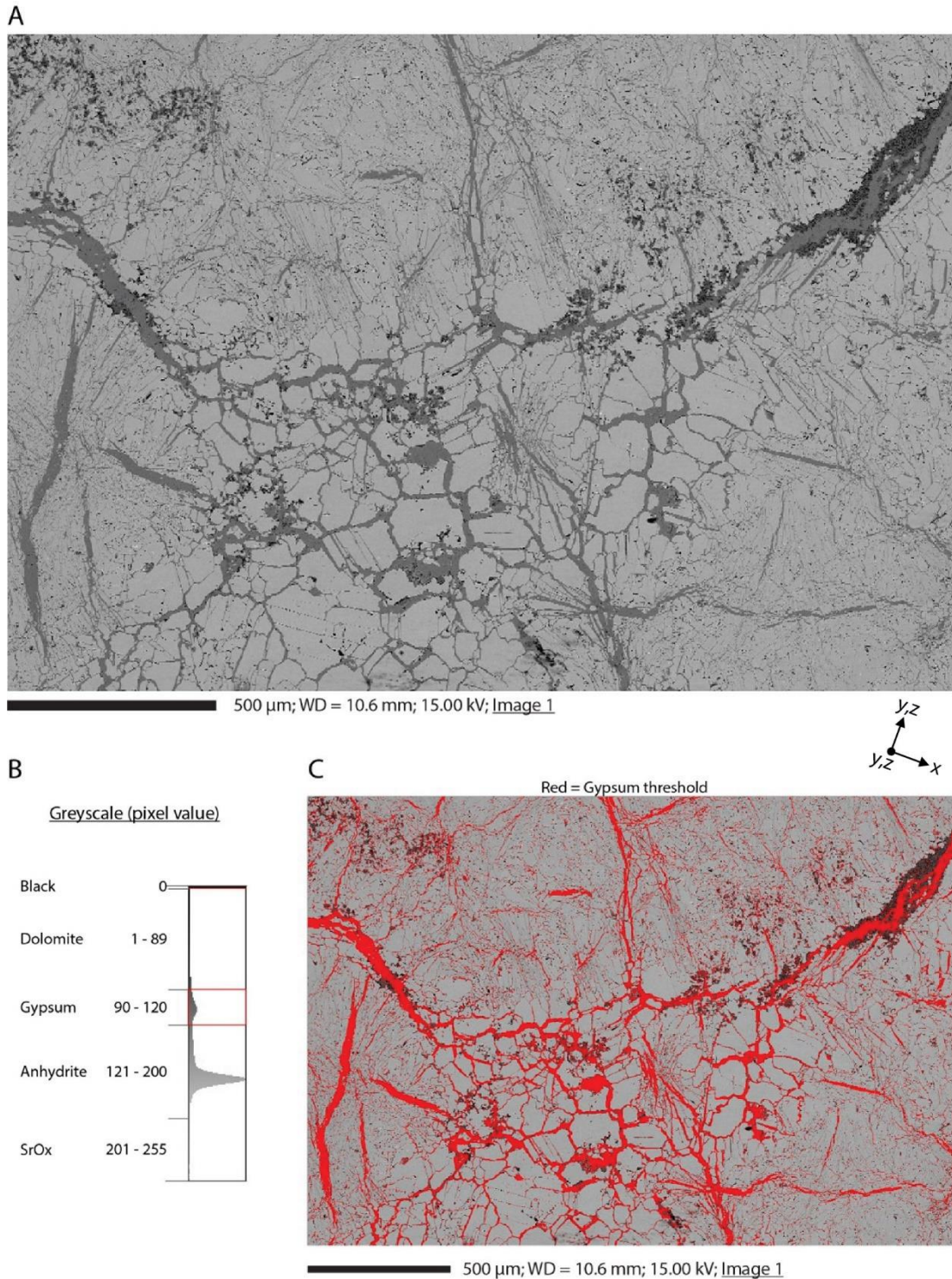


Fig. S19: Phase content analysis via greyscale threshold (ImageJ) from A: backscatter electron Image 1 of Òdena quarry sample Ò2 (BA-4) after steady state differential compaction (ssdc). The section where Image 1 was taken is from a part of the sample that shows no sign of shear fractures. B: Greyscale threshold settings defined to quantify %. SrOx = accessory phases. C: Image 1 with all pixels that fall into the gypsum threshold in red. See table A1 for further results. The location of the image is marked as 'Image 1' in Figure A11.

135

140

Table S1: Phase content greyscale threshold analysis on four backscatter electron images from two Òdena quarry samples from sections with no visible impact from deformation or hydration. Image 1 is from BA-4h (Ò2) after steady state differential compaction, but from a section that shows no sign of hydration through the experiment. Figures A16 to A19 present the Images and thresholds used for the analysis. Hal = halite, gyp = gypsum, dol = dolomite, SrO_x = accessory phases, black = open fractures. Deviation = difference between the image area and the sum of the pixels that were sorted by the greyscale threshold. SUM is the content calculated by adding phase area up, meaning that the different images were treated as one. Mean is the statistic mean of all four grey scale threshold case studies, and STDEV is the corresponding standard deviation. The marked values (bold) are the data used as initial material phase content for Òdena quarry anhydrite in the study.

	Ò8 (AA-3)			Ò2 (BA-4)					
	Image 2	Image 5	Image 6	Image 1	<i>SUM</i>	<i>Mean</i>	<i>STDEV</i>	<i>STDEV</i>	<i>STDEV</i>
Image Area [px ²]	724992	724992	724992	724992	2899968				
Image Area [µm ²]	724992.00	7080000.00	875482.57	2837203.17	11517677.74				
Anh Area [µm ²]	616855.00	5943632.86	720518.20	2283682.42	9564688.49				
Gyp Area [µm ²]	87018.00	962200.66	111973.72	403149.46	1564341.84	391085.46	406890.03		
Dol Area [µm ²]	20165.00	168674.00	39121.10	139005.57	366965.67	91741.42	73131.40		
SrO _x Area [µm ²]	96.00	175.78	227.08	5008.77	5507.63	1376.91	2421.84		
Black [µm ²]	858.00	5215.01	3654.93	6351.00	16078.93	4019.73	2379.99		
Sum [µm ²]	724992.00	7079898.32	875495.03	2837197.22	11517582.57	2879395.64	2961028.89		
Deviation [µm ²]	0.00	101.68	-12.46	5.96	95.17				
Deviation [%]	0.00	0.00	0.00	0.00	0.00083	0.00	0.00		
Anh [%]	85.08	83.95	82.30	80.49	83.04	82.96	2.00		
Gyp [%]	12.00	13.59	12.79	14.21	13.58	13.15	0.96		
Dol [%]	2.78	2.38	4.47	4.90	3.19	3.63	1.24		
SrO _x [%]	0.01	0.00	0.03	0.18	0.05	0.05	0.08		
Black [%]	0.12	0.07	0.42	0.22	0.14	0.21	0.15		

145